RADAR SIGNATURE AND SYSTEMS STUDIES AT KANSAS UNIVERSITY

by

Richard K. Moore, Director
Remote Sensing Laboratory
The University of Kansas
Lawrence, Kansas 66044

The radar signature and systems studies described here have concentrated in two areas: octave bandwidths radar spectrometry, using a truck-mounted system, and scatterometry using primarily the 13.3 GHz system on the NASA/MSC aircraft. In addition, the results of the experiments to date have been synthesized into a pair of representative designs for spacecraft radar systems—one for small spacecraft and one for large spacecraft.

Our activities in the use of radar images have been described by Haralick, McCauley and Morain, so this paper concentrates on the non-imaging systems, except in the final system design.

OCTAVE BANDWIDTH SPECTROMETRY

Responses over several octaves in the visible and infrared ranges of the spectrum have been measured for decades. In the microwave region of the spectrum, however, both active and passive systems have concentrated on single spot frequencies and measurements of continuous responses are new. We have reason to believe that the resonances that occur in nature in the microwave region will give rise to variations in response with frequency comparable in magnitude to those observed in the visible and infrared regions; but the work described here is to our knowledge the first extensive effort to determine such responses.

The University of Kansas radar spectrometer is mounted on a "cherry picker" truck that permits measurements from a height of about 12 meters. The system operates in the octave from 4 to 8 GHz, a wavelength range of 7.5 to 3.75 cm. This range was originally chosen because it was the highest frequency range for which octave bandwidth equipment is readily available. Because most of the imaging radar equipment operates at higher frequencies and because spectral responses over a wider bandwidth are desirable, the equipment is currently being extended to an upper-frequency limit of 18 GHz (1.67 cm).

The original octave bandwidth spectrometer was a pulse system that used bursts of energy 20 ns long (3 m resolution). The system was built that way so it could also be used to produce radar images in which panchromatic averaging was used. The value of the panchromatic averaging for images has now been demonstrated, and the system used in the summer of 1971 was modified from a pulse to an FM system to permit use at shorter ranges. The original pulse system would not allow vertical incidence measurements from the 12 m height, since the closest range that could be observed was about 24 m; the new system is useable at ranges as short as 5 m.

Figure 1 shows a block diagram of the system currently in use. The signal is obtained from a standard sweep oscillator and amplified to a level as high as 20 watts. The output of the amplifier is leveled with a feedback loop. The signal is transmitted through an appropriate circulator, but a sample of the signal is fed into a mixer where it is combined with the received signal. Because the transmitted signal has changed frequency during the time for the wave to travel from the antenna to the ground and back, the mixer observes two different frequencies: the one being transmitted and the one that was transmitted a short time before. The difference frequency for these experiments was set at 37 kHz; this difference frequency was amplified and filtered and the output observed on a voltmeter. Averaging was achieved by sweeping over a bandwidth of approximately 0.4 GHz for each measurement. The center frequency for the sweep was stepped between measurements.

Measurements were made during July of 1971 at more than 80 fields in the vicinity of Lawrence, Kansas. Different orientations were used relative to the rows of crops so that the effect of look direction could be established.

The system was calibrated by measuring the return from a metal sphere suspended by nylon string from the guy wire of a radio station. Because of some doubt regarding the accuracy of this calibration, the data presented have been normalized to the data observed for returns from cornfields since more cornfields were sampled than fields of any other crop.

Figure 2 shows the variation with angle at a frequency near the bottom of the band of the instrument. Since normalization is with regard to corn, corn shows no variation, whereas the other crops observed—soybeans, alfalfa and sorghum—do show an angular variation. This sort of curve is similar to that obtained by the usual single frequency scatterometer. Notice the difference between the shape of the curves for horizontal and vertical polarization.

Figure 3 shows similar curves at 5.8 GHz, and Figure 4 shows the result at 7.4 GHz near the top of the frequency band of the instrument. Variations in the angular behavior at the different frequencies are apparent. The data are still being examined for consistency and for interpretation of these variations.

Results like those shown in Figures 2, 3, and 4 could have been obtained with fixed frequency scatterometers, although in this case the broad bandwidth permitted better averages at each angle than would have been possible with narrow bandwidth systems. Figure 5 shows the variation across the band as a function of frequency—a type of presentation possible only with the octave bandwidth system. Again, note the difference between the shape of the curve for vertical and horizontal polarization, and note also that at this angle of incidence (30°) the sorghum is uniformly low but not too different from the corn for horizontal polarization, whereas alfalfa peaks somewhat below the middle of the frequency range but is lower on both sides and soybeans are low at low frequencies but higher at the high frequency end. The variations are not as pronounced for vertical polarization, but they are present there too.

Figure 6 shows similar results plotted for an incidence angle of 50°. Notice that at this incidence angle the trends are different and the variations for vertical polarization are considerably more striking than at the steeper incident angle.

These results are only samples; the data are still being analyzed. Measurements were made at angles from vertical incidence (0°) to 70°, and the angular curves could have been plotted for each of the frequencies shown as points on the spectral curve.

A major purpose of the broad spectrum measurements is to illustrate the potential for polypanchromatic radar systems, i.e., for radars that attain averaging of the phase interference effects by panchromatic transmission, but split up the panchromatic band into segments to achieve spectral signatures. Observation of the curve of Figures 5 and 6 shows that some differences do exist, but a more striking illustration is obtained by using the mean of each one-third octave to set the brightness of one of the three primary colors (red, green, and blue), and combining these colors to achieve a resultant color characteristic of the particular spectral response. Figure 7 shows the result obtained by such color combination at four different angles for soybeans. Note that for vertical polarization the colors are all about the same—red—although there is significant difference for each angle for horizontal polarization. The problem for vertical polarization is that all the soybean echoes peak at the low frequency end of the spectrum. To obtain a greater variability the spectral response was normalized relative to the average for all crops at a given angle, and the deviation from this average used to determine the color in each one-third octave band. Figure 8 shows what this does to the colors of Figure 7. Here not only have the colors for the horizontal polarization been changed, but there is some variation showing for vertical polarization. With the soybeans for the steeper incidence angles, however, the result is always white; that is, the variation across the band is small. Figures 9 and 10 show the similar result for 30° and 50° for all four crops. Clearly at either angle distinctions could be made between the crops on this basis if both polarizations are available, although at 30° horizontal polarization does not permit distinction between sorghum and soybeans, and vertical polarization between sorghum and alfalfa. At 50° with horizontal polarization, soybeans and alfalfa are the same, and with vertical polarization only alfalfa is different. Thus it appears that, in this part of the frequency range, both polarization and frequency are necessary to separate the crops; but the separation is quite adequate at each angle when both polarizations are used.

These results must be considered preliminary and further analysis may show that they are not completely consistent so that more data will have to be collected. Nevertheless we do believe that they show the potential of polypanchromatic systems and, indeed, final analysis of the data from July 1971 may verify the conclusions one can draw from these illustrations.

OCEANIC SCATTEROMETRY

A major effort has been expended over the last three years to evaluate fully the operating problems and capabilities of the 13.3 GHz scatterometer system flown on the MSC aircraft. Some of the reports issued dealing with analysis of the data and of the system itself are shown in Figure 11. Other reports have not been formally designated but have been provided to MSC in letter form or over the telephone, and still further analyses are being completed. We believe that the system can be considered reliable for measurement of the ratio of scattering coefficients at two angles for any given year, although differences exist from year to year because of changes in the antenna pattern caused by handling and more particularly by the change from the P3 aircraft for Missions 88 and 119 to the C130 aircraft for Mission 156. Data analysis techniques have been developed to compensate for these effects as much as possible.

Under a contract with the Naval Ordnance Laboratory, The University of Kansas has developed a scatterometer system of its own which has been flown this past year in a University aircraft. Figure 12 shows a photograph of the system mounted in the passenger compartment of the University aircraft. The two units on the left with handles visible are the scatterometer and its measuring instruments; the rest of the equipment shown has to do with the tape recorder which appears at the bottom of the illustration. This instrument has now flown both in the Arctic north of Alert and near Thule, and in Kansas, including the Garden City test site. Figure 13 shows representative data obtained from these missions. Further analysis of these data is continuing.

The major effort in recent years with the NASA/MSC scatterometer has been to collect and analyze oceanographic data. Because of possible variations in the calibration of the system, data have all been normalized to the scattering coefficient measured at 10°. This is a procedure that eliminates all effects of gain changes or changes in the calibration signal "constant." The analysis of the system shows that the calibration constant may in fact vary from mission to mission, although it should remain fixed during a particular mission.

Other potential error sources exist in the data reported here. A major source of error is knowledge of the windspeed itself. Even for the flights near the Argus Island tower, there is uncertainty about the windspeed, as described by Pierson and Moore in another paper in this meeting. Although the aircraft attitude is recorded when the ADAS is operating satisfactorily, error in this recording could cause use of the wrong gain value because of rapid fluctuations in the antenna pattern with depression angle. On some missions the ground speed measurement with the Doppler navigator on the aircraft appears to be inaccurate, and in fact some of the flight lines were made with estimates rather than with the Doppler measurement because of a failure of the Doppler system. Such an error in ground speed causes assignment of the scattering coefficient measured at a particular frequency to the wrong angle, which has the dual effect of showing it at the wrong angle and of causing use of the wrong antenna gain.

The effect of these potential error sources is believed to be random and to result in a scatter of points about the regression line. Nevertheless, the scatter is relatively small in terms of percentage of the wind speed or the measured scattering coefficient value. We are quite encouraged by the results.

Figure 14 shows the normalized scattering coefficient plotted versus the wind speed on a log-log plot for 35° incidence angle and the upwind direction. Note that the points for Mission 156 were raised 1.6 dB. The need for this is believed due to the change in the antenna pattern in moving the scatterometer from the P3 to the C130 aircraft. The dash-lines show the rms error about the regression line. The scattering coefficient varies approximately proportional to the 1.4 power of wind speed. There has been some discussion about the two points at 49 kts lying beneath the 1σ value. However, Figure 15 shows the same result for 25°, and the points for 49 kts at this angle lie almost exactly on the regression line. Thus we believe the 35° points may be partly in error due to some lack of knowledge of aircraft attitude and should not be construed as proving that some sort of "saturation" takes place.

Crosswind data are shown in Figure 16 for 35°. Here the 49 kt points lie above the regression line. Crosswind data for 25° are shown in Figure 17 where again the 49 kt points lie rather high. Notice that at 25° the wind speed variation for

both upwind and crosswind is significantly less than it is at 35°, and that for crosswind the variation is less than for upwind.

A similar analysis has been conducted of Naval Research Laboratory observations available to us, namely those from JOSS I in 1970 and from the North Atlantic mission conducted from Ireland in 1969. Figure 18 shows a sample of the kind of variation observed for the NRL data where the points from the two missions have been separately fitted to regression lines. The regression lines have somewhat different slopes, but nevertheless they both show a variation significantly greater than linear. In our analysis of the NRL data, we have used the same technique that was used with the MSC data; that is, these two regression lines have been brought together at 20 kts and all the points on the lower line have been moved up by the amount necessary to make the lines intersect at that point. When this new cluster of points has been plotted, the modified points have been used in the regression program to obtain a new composite regression line.

The results of these analyses of NRL data are summarized in Figure 19 where the exponent in a power law variation of scattering coefficient with wind speed is plotted. The downwind data appear somewhat more consistent than the upwind data, but in both cases the scattering coefficient variation with wind speed is at least linear. Notice that for horizontal polarization and larger incidence angles the variation of scattering coefficient with wind speed approaches a square law. This indicates that horizontal polarization is superior to vertical polarization for radar anemometry of the sea, but it must be balanced against the weaker signal return for the horizontal signals for moderate seas and the consequent increase in required power.

Since the radar data is to be applied to anemometry, we felt it appropriate to plot "anemometer calibration curves" for our own and NRL data for the different angles, directions, and polarizations. In this case, the wind speed is the dependent variable and the scattering coefficient is the independent variable. Figures 20, 21, 22 and 23 show the MSC data plotted this way for upwind and crosswind for 35° and 25° again with the 1σ error bars shown alongside the trendlines. A better anemometer has a more nearly horizontal calibration line because this means that a larger variation in scattering coefficient is required to indicate a small variation in wind speed. Similar plots have been made for the NRL data; two samples are shown in Figures 24 and 25 for 60° upwind with horizontal and vertical polarization. Clearly the horizontal polarization, since it is significantly less steep than the vertical polarization, will make an anemometer less sensitive to errors in the measurement of the scattering coefficient.

A significant difference was noted between the North Atlantic and Bermuda missions, both for the MSC and for the NRL data. With the NRL data, we see no solid instrumental reason to expect this variation, although one can easily rationalize it in terms of changes in the MSC antenna pattern. It may be that other factors will have to be taken into account in using radar for anemometry, for instance the air/sea temperature differences or differences in the surface tension in different parts of the ocean. Presumably the further experimentation being conducted using the S193 Skylab experiment can answer some of these questions much better than any aircraft program making measurements in different parts of the ocean on different years.

ICE SCATTEROMETRY

Although an aircraft scatterometer may have operational application over the Arctic ice, a spacecraft scatterometer or radiometer will have such a poor resolution that it can only be used for gross measurements in the polar regions (or anywhere else for that matter). Thus, one of the major purposes of the scatterometer over the ice, as well as over land, is to determine the sensitivity and dynamic range required for a radar imager. Since the imager will be able to operate with fine resolution from spacecraft altitudes, it definitely is the preferred sensor for the ice.

The data from Mission 126 have been analyzed with this in mind. Figure 26 shows the spread of the average scattering coefficient for nine different ice types as a function of angle of incidence. Figure 27 shows this converted into dynamic range requirements for the ice imager. Clearly an imager operating at steep angles of incidence required wide dynamic range from about -12 to +15 dB; whereas an imager whose closest angle of incidence is only about 35° can get by with a dynamic range of considerably less than 20 dB as shown, but must have a sensitivity at least of -14 dB. Analysis of these data along these lines is continuing.

AGRICULTURAL SCATTEROMETRY

Figure 28 summarizes the agricultural scatterometry program. Unfortunately we have not received any complete data sets from the missions flown in the summer of 1970 or 1971. Preliminary data were received from Mission 130, flown in 1970, as requested. These were used during the summer of 1971 to establish improved format specifications for processing the remainder of the scatterometer data. By a preliminary examination of one line, it was possible to specify the most efficient use of the computer time for agricultural scatterometry. Also specified was the need for the automatic data output plot to be scaled so that it could be directly overlaid on a photographic mosaic. The data processing sample length was specified and the angular resolution frequency band required was also specified.

The 400 MHz scatterometer data flown in 1970 over the Garden City test site have been received and are being analyzed. No results are available yet.

SATELLITE RADAR SYSTEM

The major goal of our program is specification of appropriate satellite radar systems and their applications. This paper closes with a discussion of two representative systems which might be flown on satellites. These systems are not to be considered as final specifications; they could be modified in many ways depending upon the constraints associated with the satellite.

Figure 29 shows the specifications for a radar for a small satellite capable of supplying 450 watts of power. With this much power the system could have a resolution as fine as 10 m with a swathwidth of 40 km. To achieve this large swathwidth, however, requires erecting an antenna on the small satellite with a length of the order of 6 to 10 m. Note that if the radar is only used 20% of the time, the average power over an orbit is only 90 watts. The system was selected to operate out to an incidence

angle of 60° for geologic purposes. A 30° incident angle appears quite adequate for agricultural purposes and many geologic purposes. With such an incident angle the power requirement could be reduced to 275 watts, which means that the average over an orbit is only 55 watts.

Such a system would, we assume, transmit raw video data to the ground via a wideband telemetry link. Processing would then take place on the ground. The power for the telemetry link is not included in the figure. Of course, a system with a poorer resolution could get by with significantly less power for both radar and telemetry.

Figure 30 shows a possible system for a large satellite such as a shuttle. Here a polypanchromatic system is postulated with first the power required with no averaging, then that with 200 MHz, and then with 400 MHz averaging. The 200 MHz averaging gives about 10 independent samples per cell due to panchromatic illumination and the 400 MHz gives about 20 per cell. Note that this 4-frequency system requires a total of 975 watts without averaging, but with 10 independent samples per cell the power requirement goes up by a factor of about 10. The frequencies were chosen somewhat arbitrarily because we still do not have adequate data over a wide range. However, 16 GHz appears about the highest reasonable frequency for a spacecraft imaging system both from the standpoint of available components and of atmospheric effects. The 10 GHz band is quite common and many data have been gathered at this frequency that indicate the value of radar. Our recent observations over the octave bandwidth indicate that the 4 and 8 GHz regions are also useful. All of these frequencies are near to frequencies that may be available for allocation for imaging radar systems.

As our analysis of the observations both with the imaging radars and the radar spectrometer and scatterometer continue, we hope to be able to refine these specifications. Nevertheless we believe if a radar system could be constructed for spacecraft use immediately, these specifications could serve as a reasonable guide.

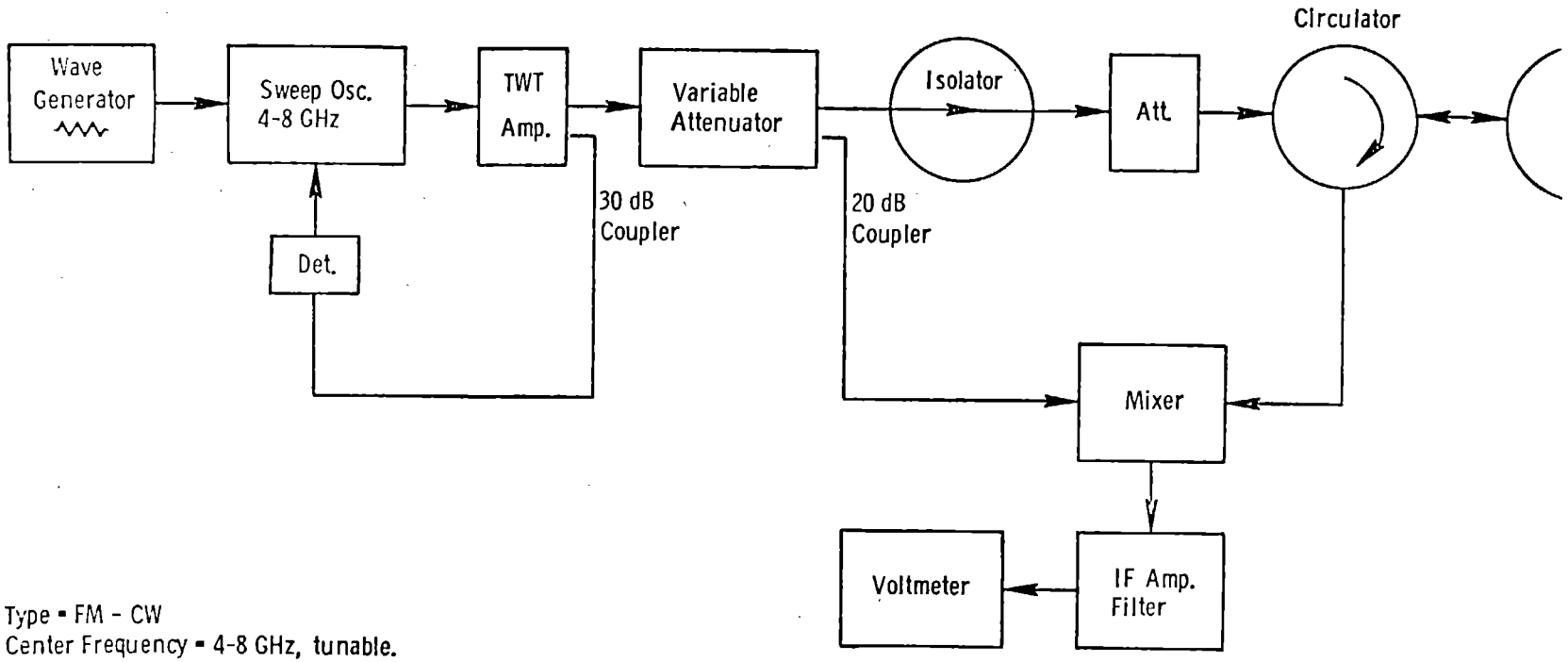

Type = FM - CW
Center Frequency = 4-8 GHz, tunable.
Modulation Bandwidth = 400 MHz
IF Frequency = 37 KHz
Antenna = 3' diameter dish

Figure 1. Block diagram of FM-CW Octave-Bandwidth Radar Spectrometer.

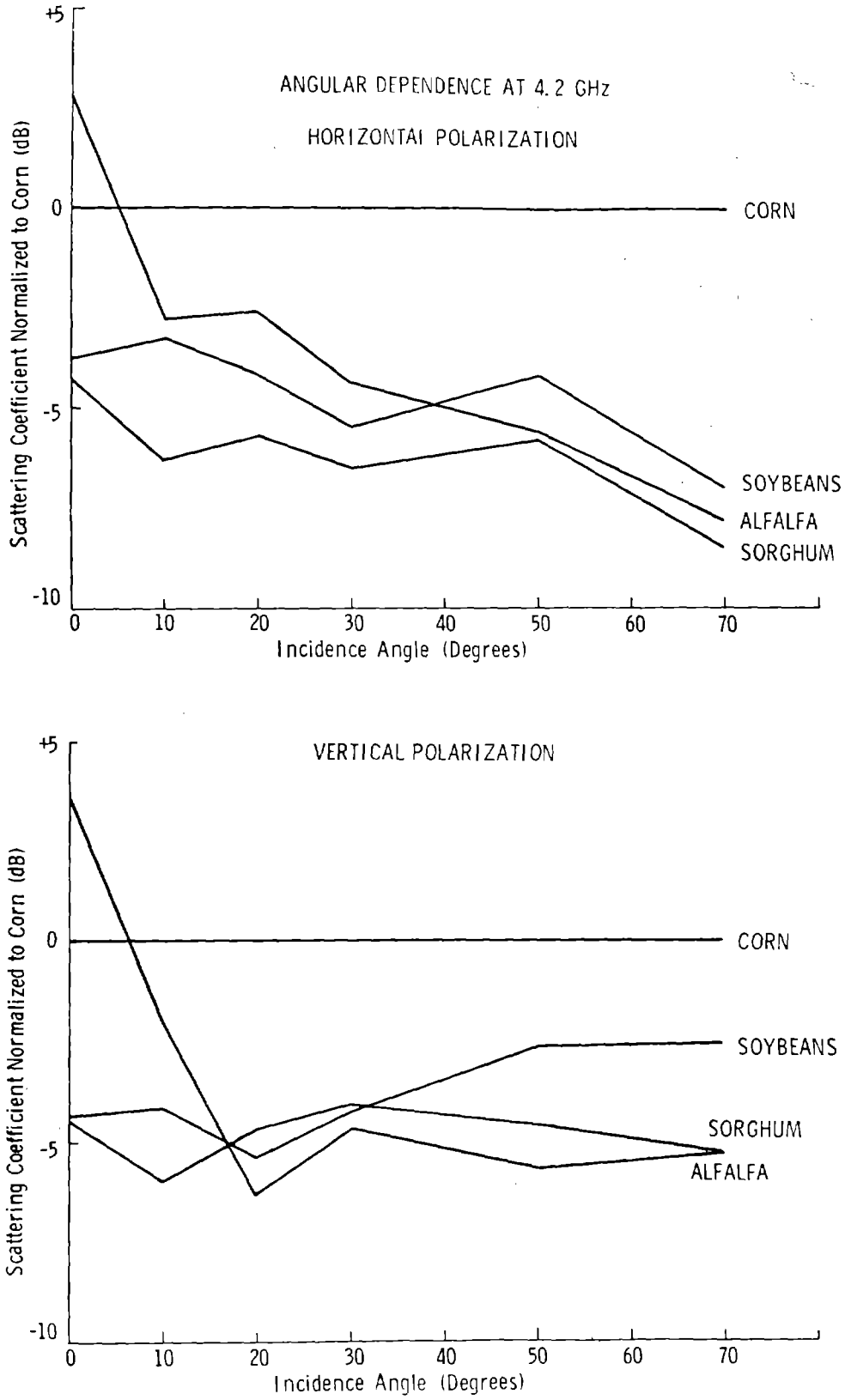

Figure 2. Example of single-frequency observations of radar backscatter, July 1971.

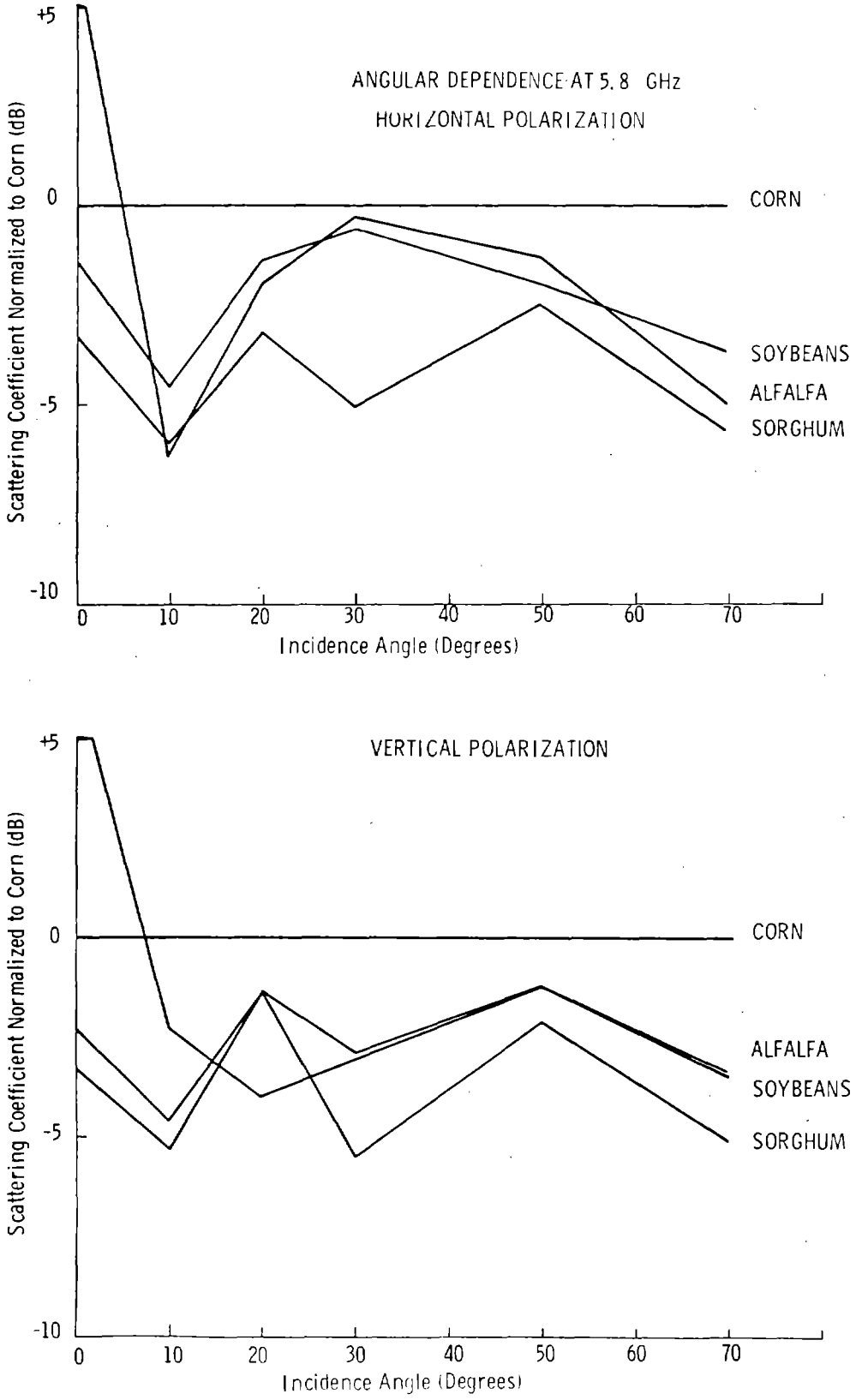

Figure 3. Example of single-frequency observations of radar backscatter, July 1971.

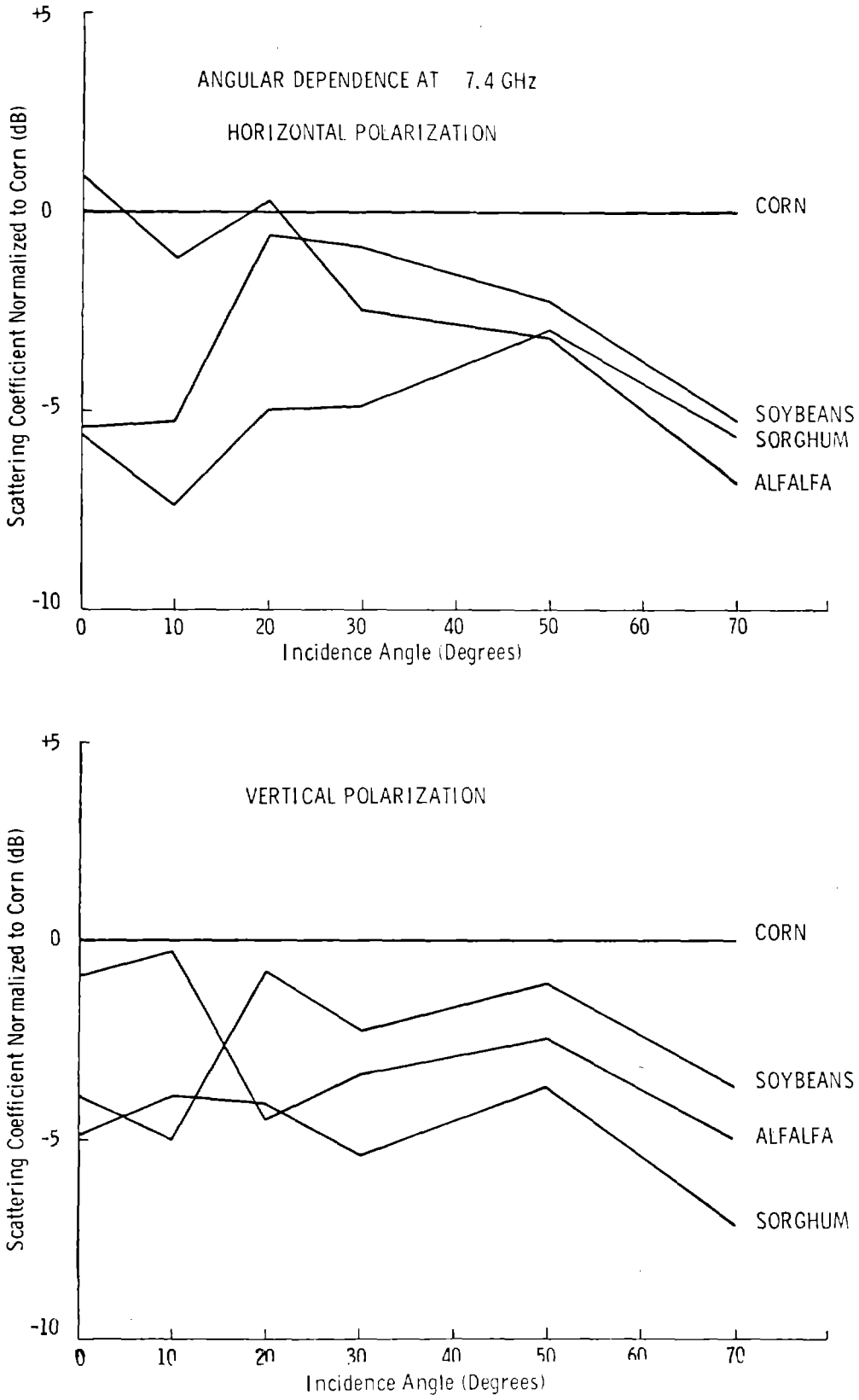

Figure 4. Example of single-frequency observations of radar backscatter, July 1971.

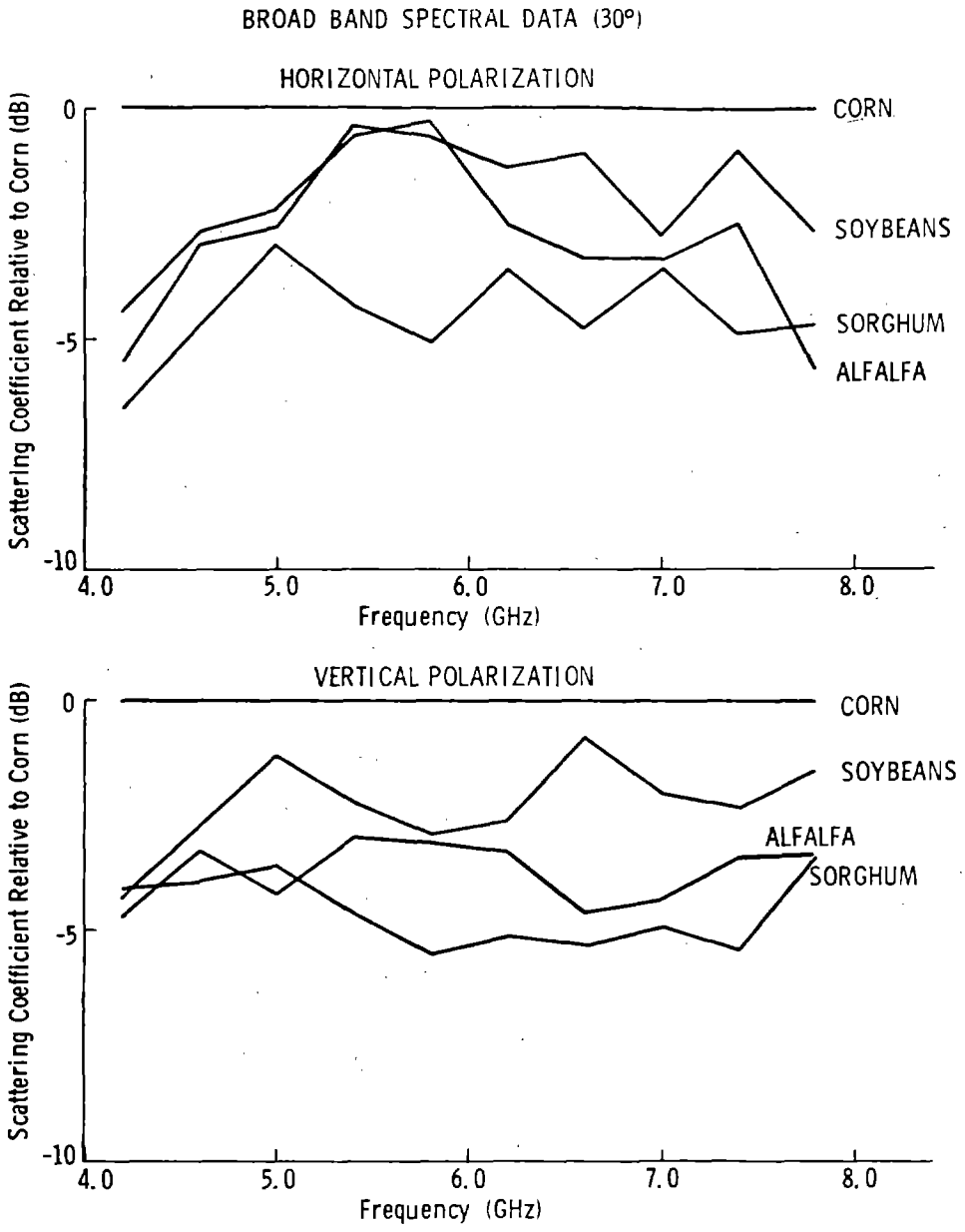

Figure 5. Example of radar spectral response, July 1971.

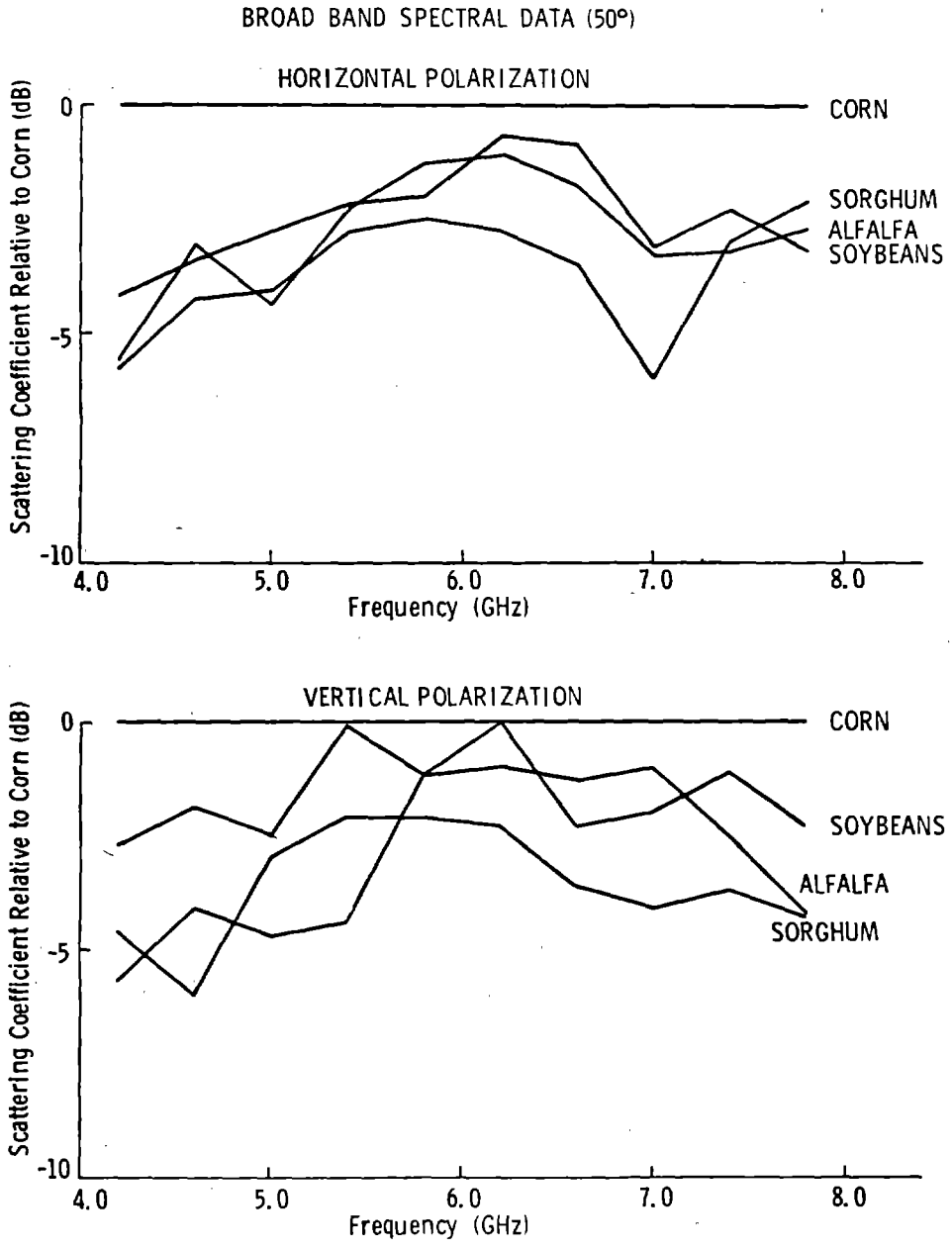

Figure 6. Example of radar spectral response, July 1971.

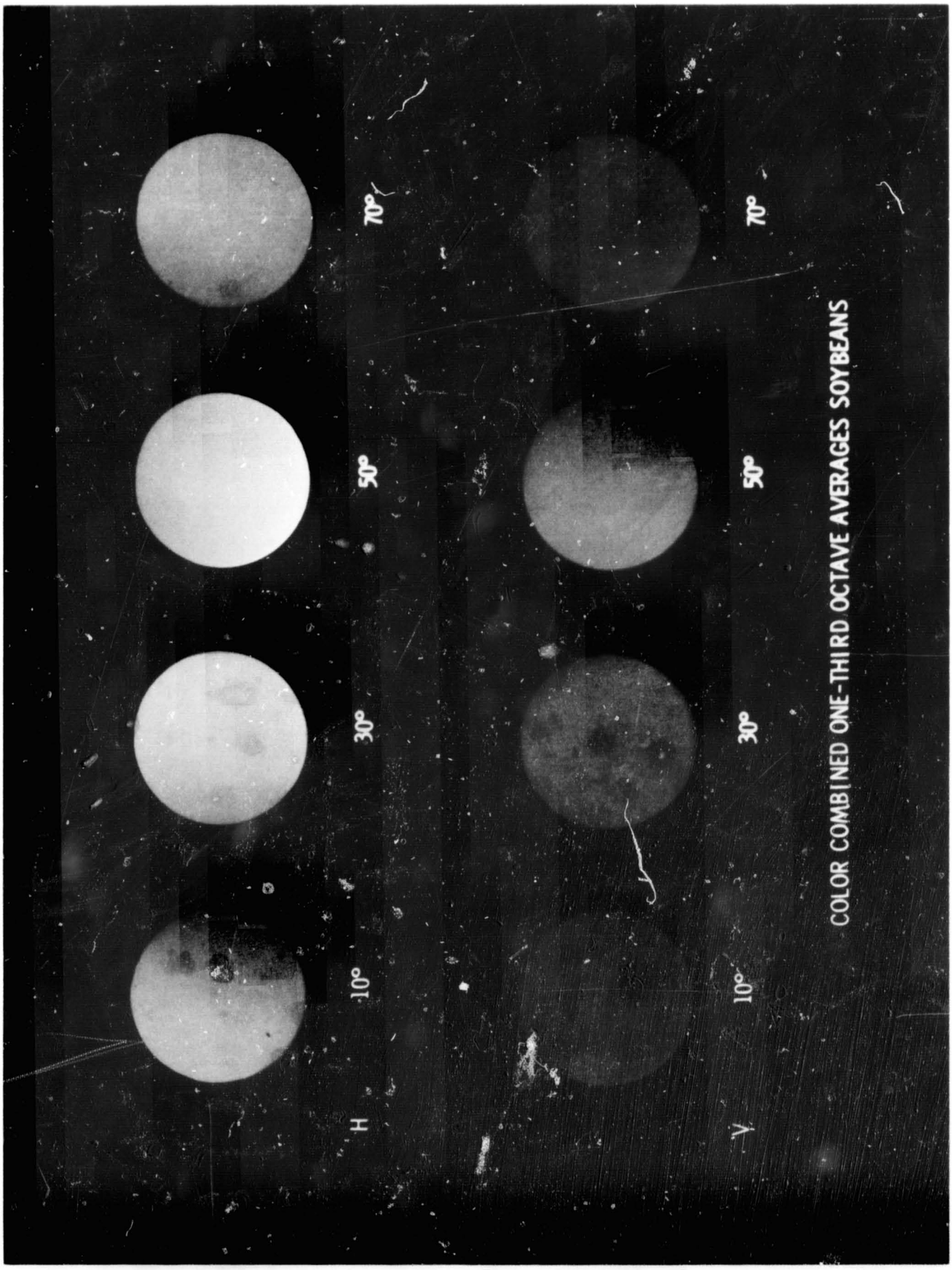
COLOR COMBINED ONE-THIRD OCTAVE AVERAGES SOYBEANS
H
V
10°
30°
50°
70°
10°
30°
50°
70°

Figure 7.

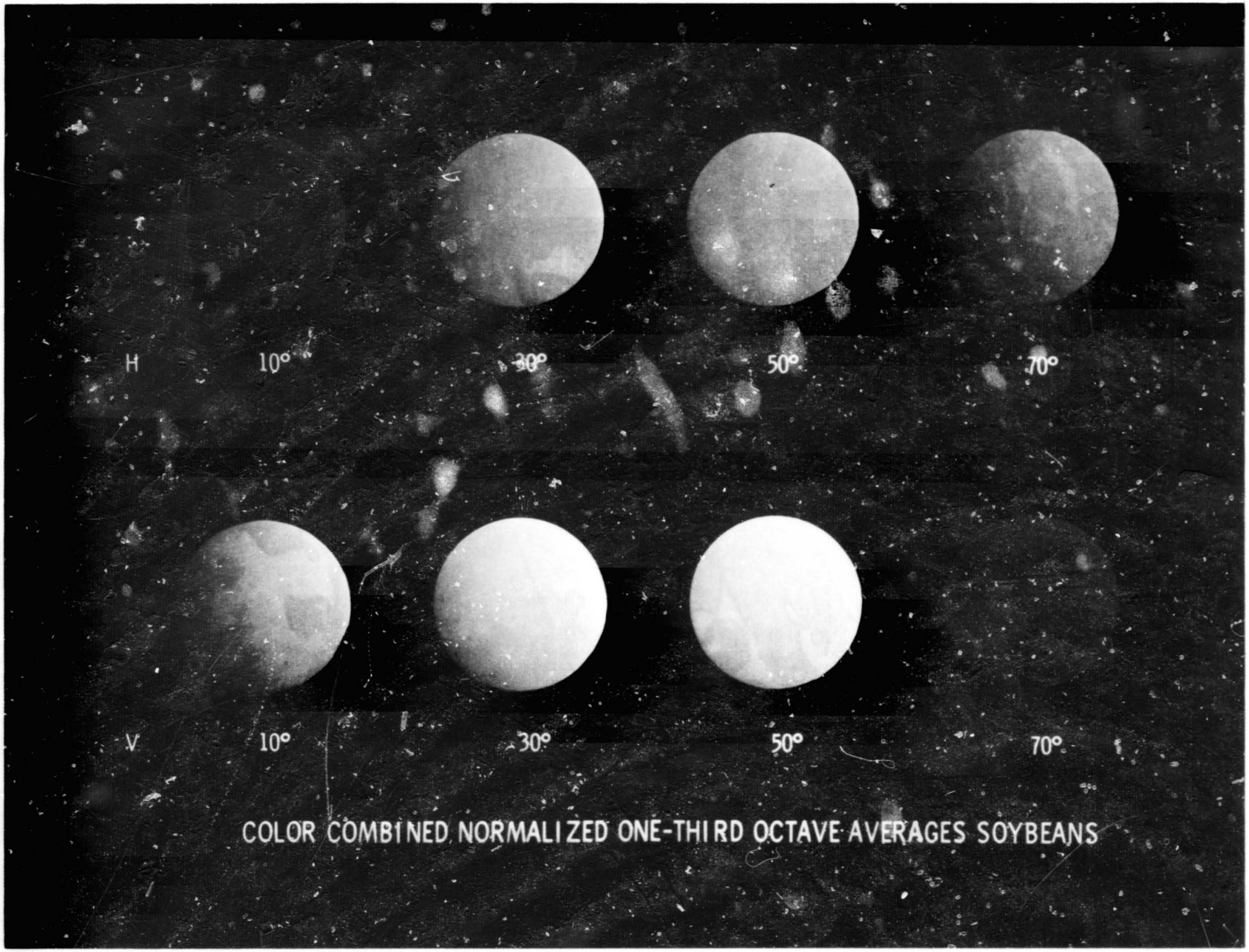
H
10°
30°
50°
70°
V
10°
30°
50°
70°
COLOR COMBINED NORMALIZED ONE-THIRD OCTAVE AVERAGES SOYBEANS

Figure 8.

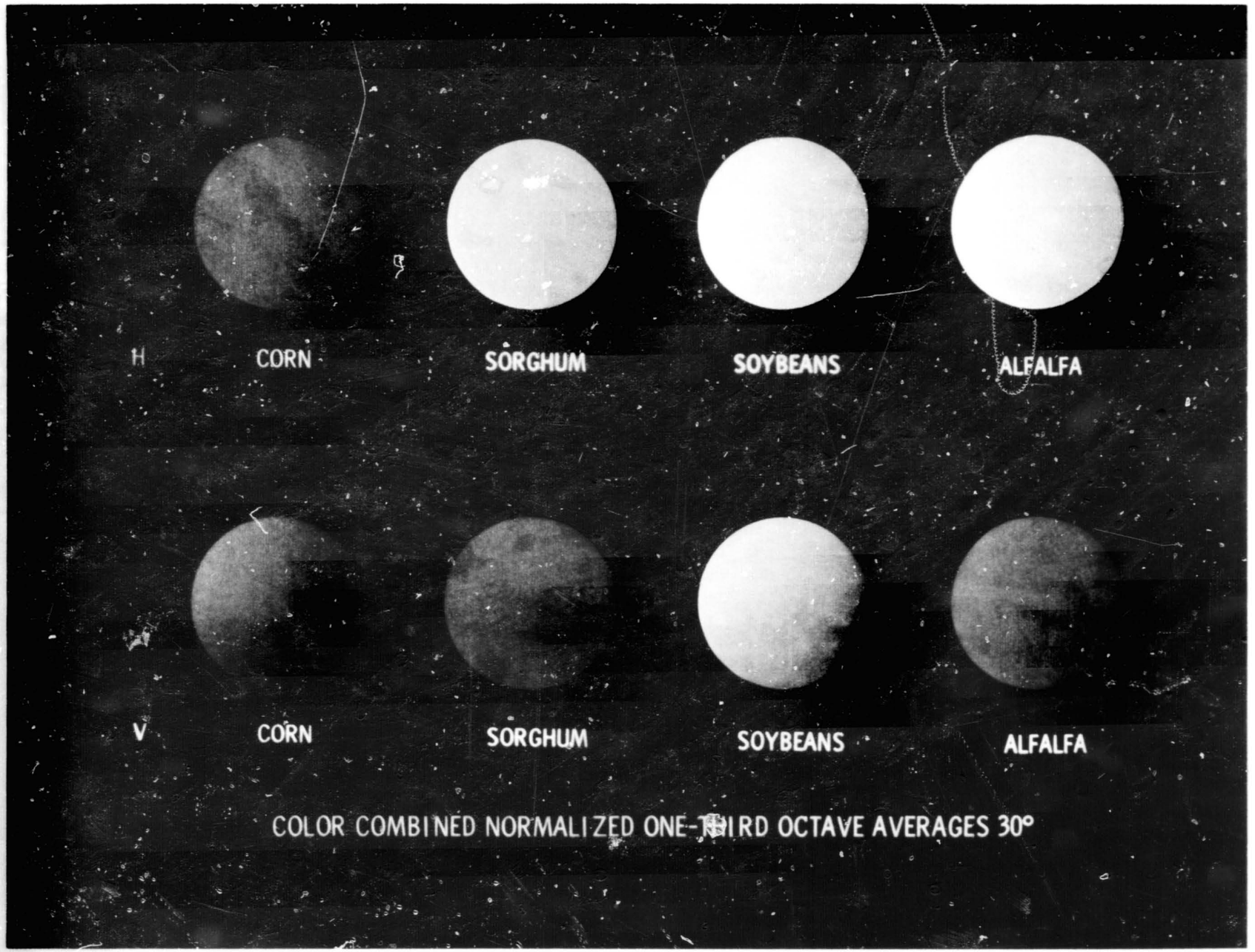
H
CORN
SORGHUM
SOYBEANS
ALFALFA
V
CORN
SORGHUM
SOYBEANS
ALFALFA
COLOR COMBINED NORMALIZED ONE-THIRD OCTAVE AVERAGES 30°

Figure 9.

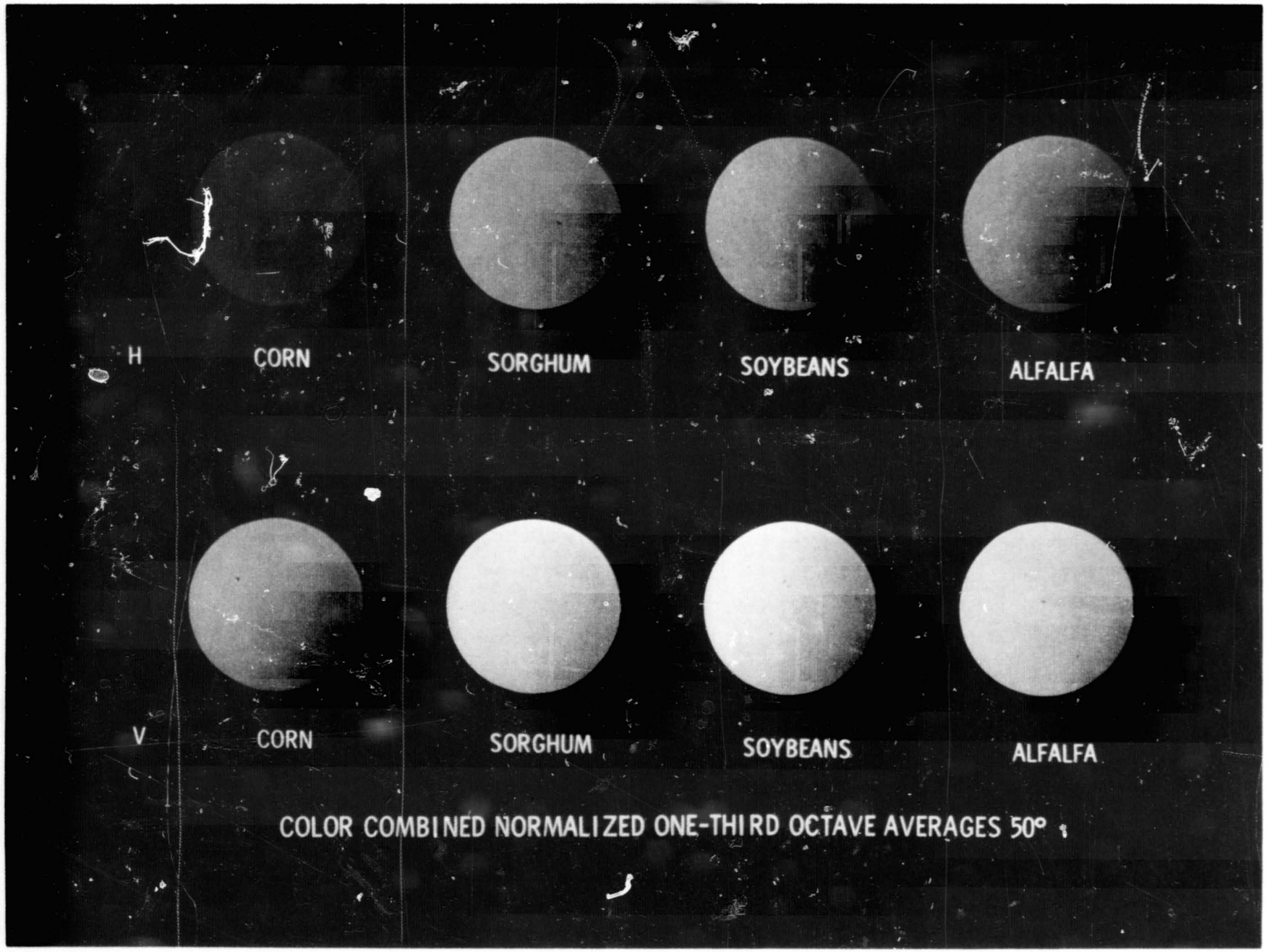
H
CORN
SORGHUM
SOYBEANS
ALFALFA
V
CORN
SORGHUM
SOYBEANS
ALFALFA
COLOR COMBINED NORMALIZED ONE-THIRD OCTAVE AVERAGES 50°

Figure 10.

13.3 GHz SCATTEROMETER SYSTEM ANALYSIS

"THE EFFECT OF AMPLIFIER SATURATION ON A DOPPLER SCATTEROMETER," TECHNICAL REPORT 118-17.

"POST-FLIGHT OPERATIONAL ANALYSIS OF THE NASA 13.3 GHz DUAL-POLARIZED RADAR SCATTEROMETER—NASA/MSC AIRCRAFT MISSION 102, SITE 76, GARDEN CITY, KANSAS, FLIGHT DATE: 3-4 SEPTEMBER 1969," TECHNICAL MEMORANDUM 118-18.

"AN ANALYSIS OF RF PHASE ERROR IN THE 13.3 GHz SCATTEROMETER," TECHNICAL MEMORANDUM 177-1.

"AN ANALYSIS OF METHODS FOR CALIBRATING THE 13.3 GHz SCATTEROMETER," TECHNICAL REPORT 177-1.

"SIGNAL ANALYSIS OF THE SINGLE-POLARIZED 13.3 GHz SCATTEROMETER," TECHNICAL REPORT 177-2.

"AN ANALYSIS OF THE EFFECTS OF AIRCRAFT DRIFT ANGLE ON REMOTE RADAR SENSORS," TECHNICAL REPORT 177-5.

"A NOTE ON THE ANTENNA BEAMWIDTH TERM USED IN THE SCATTEROMETER DATA REDUCTION PROGRAM," TECHNICAL MEMORANDUM 177-13.

Figure 11. Reports describing analysis of 13.3 GHz radar scatterometer system.

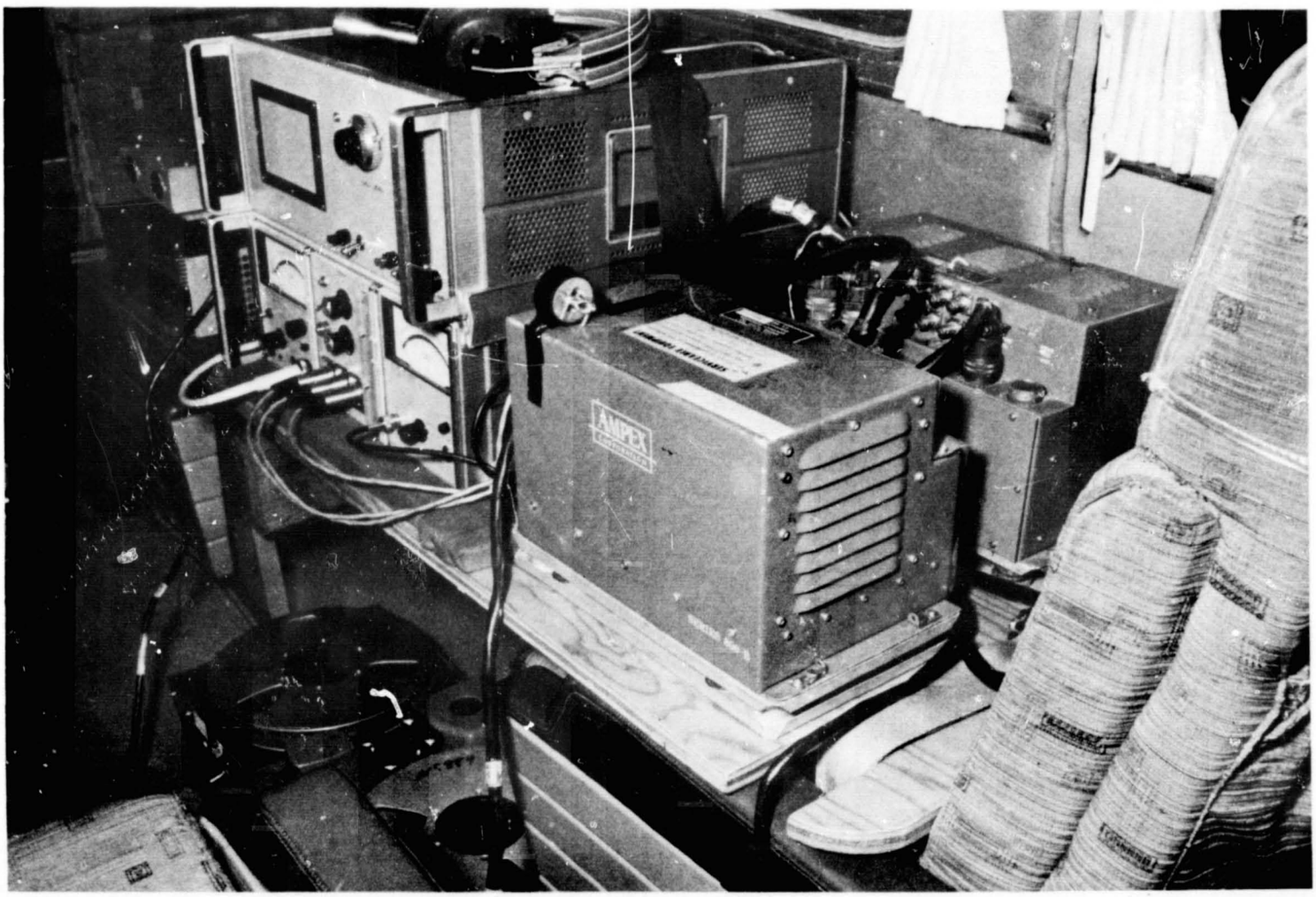

Figure 12. Kansas University 9.3 GHz radar scatterometer mounted in passenger compartment of C-45 aircraft. Scatterometer units beneath headphones; other units are parts of recorder.

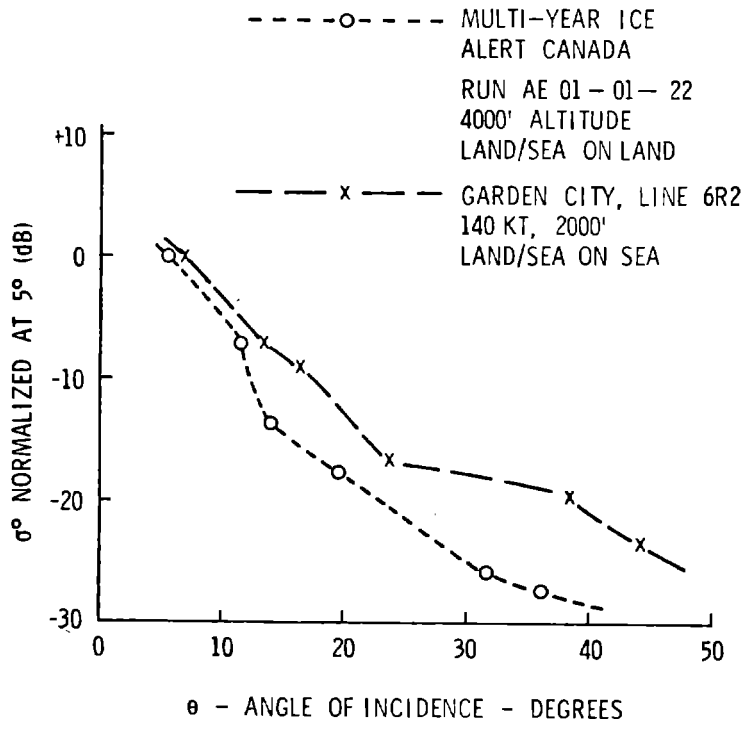

Figure 13. Kansas University 9.375 GHz scatterometer. Preliminary data.

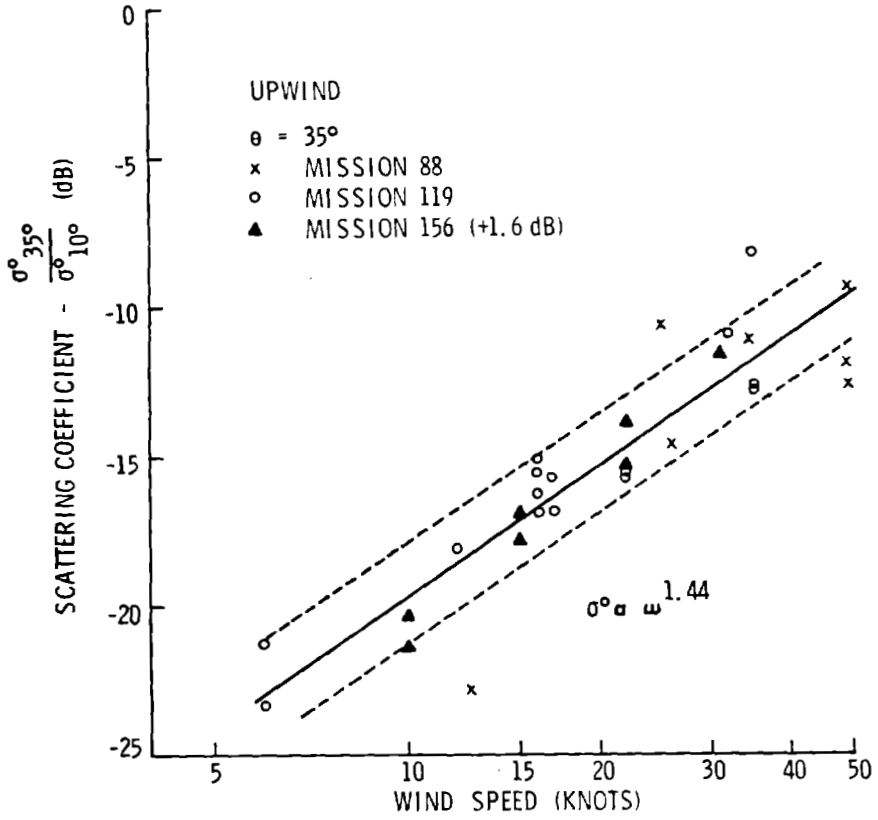

Figure 14. Oceanic scattering at 13.3 GHz 35° upwind.

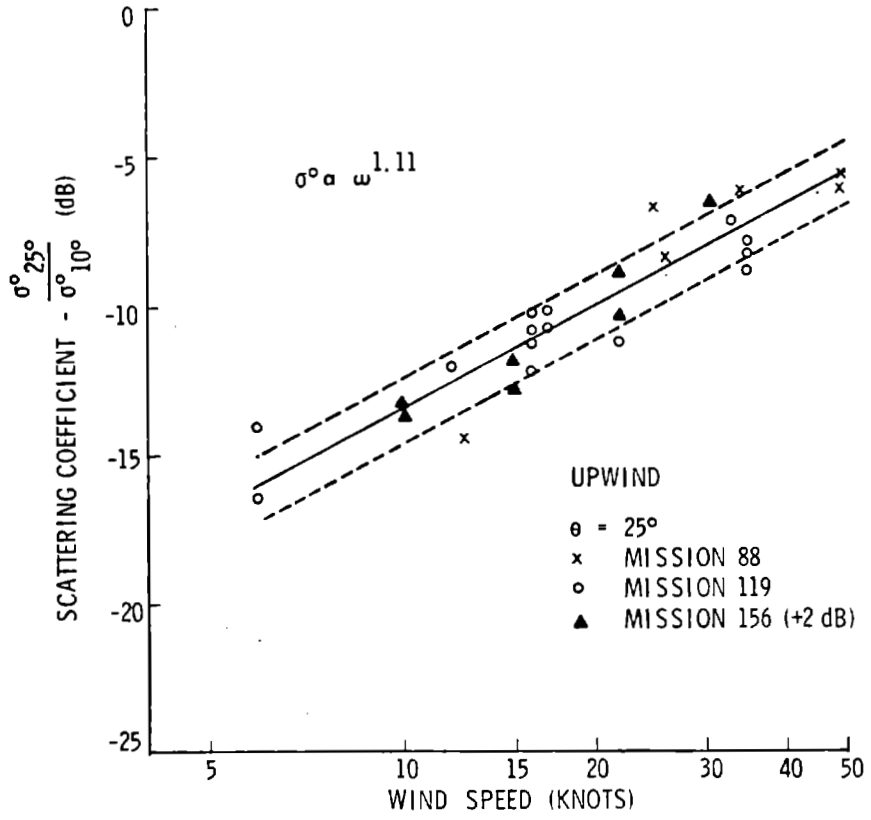

Figure 15. Oceanic scattering response at 13.3 GHz 25° upwind.

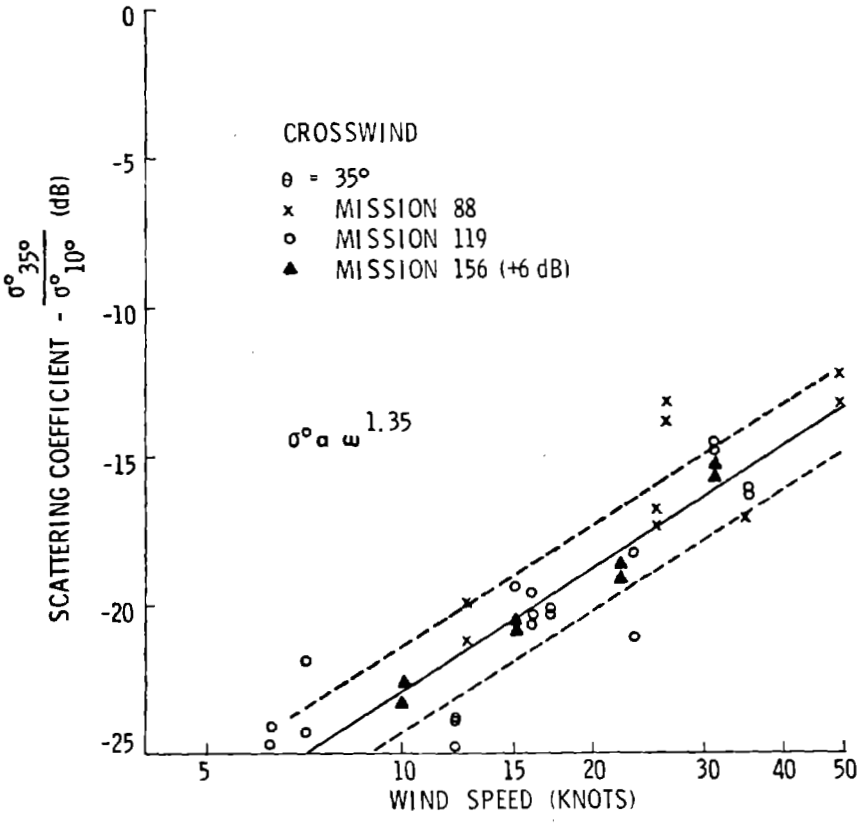

Figure 16. Oceanic scattering response at 13.3 GHz 35° crosswind.

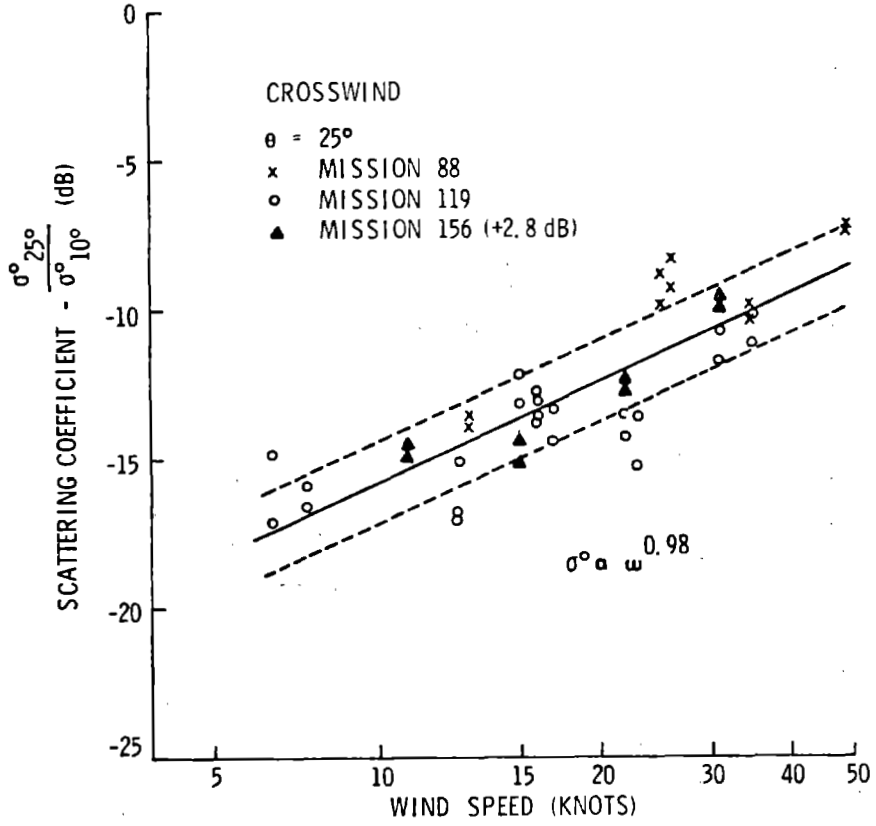

Figure 17. Oceanic scattering response at 13.3 GHz 25° crosswind.

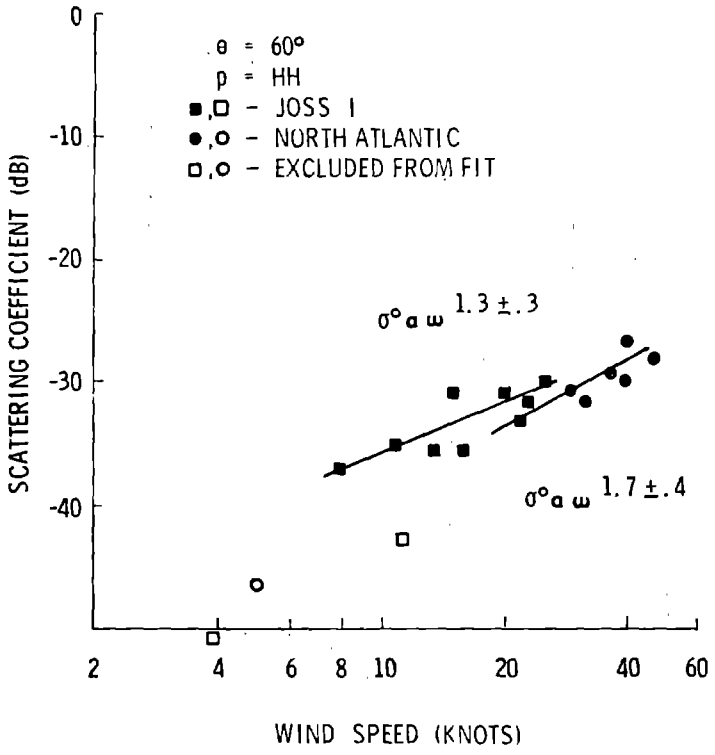

Figure 18. Oceanic scattering response at 8.9 GHz. NRL data showing separate regression lines for two missions.

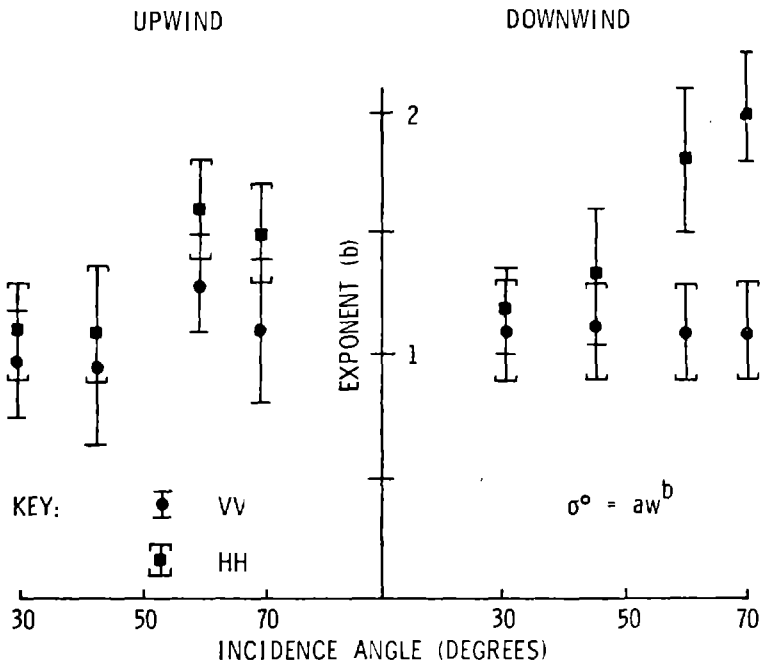

Figure 19. Power law character of NRL X-band data after adjustment.

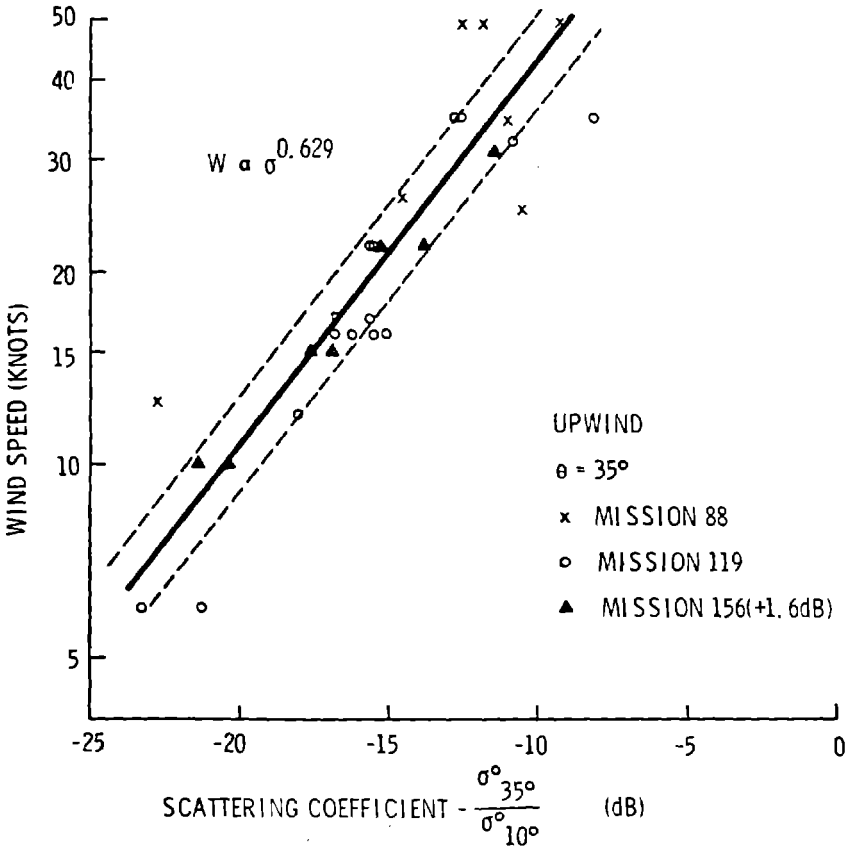

Figure 20. Anemometer calibration curve 13.3 GHz scatterometer 35° upwind.

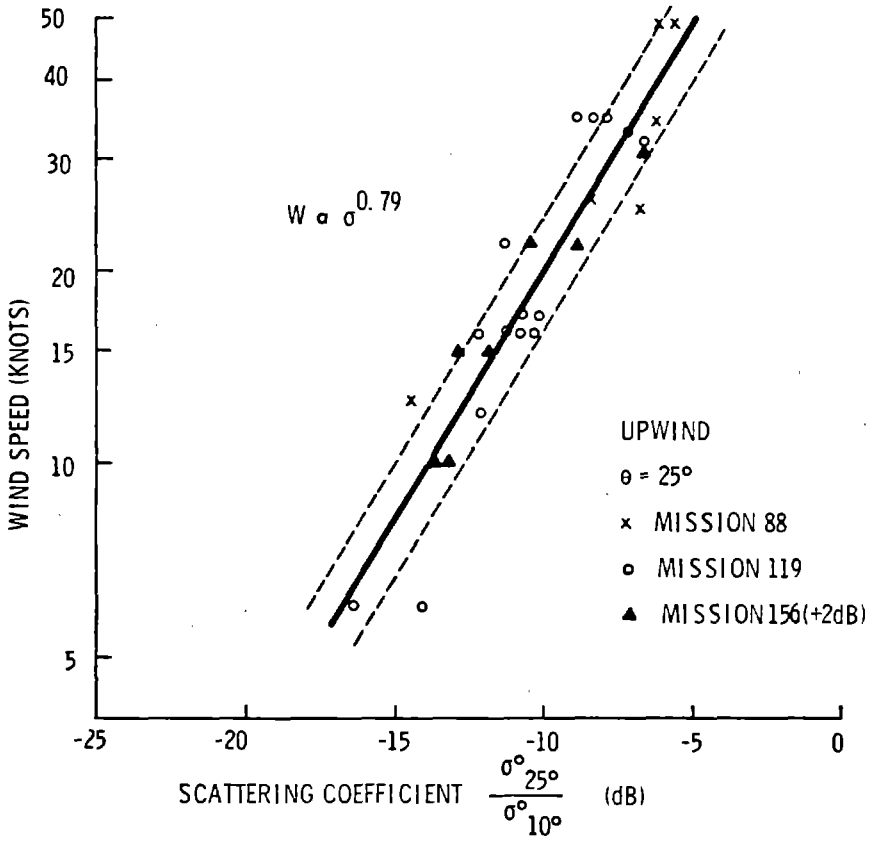

Figure 21. Anemometer calibration curve 13.3 GHz scatterometer 25° upwind.

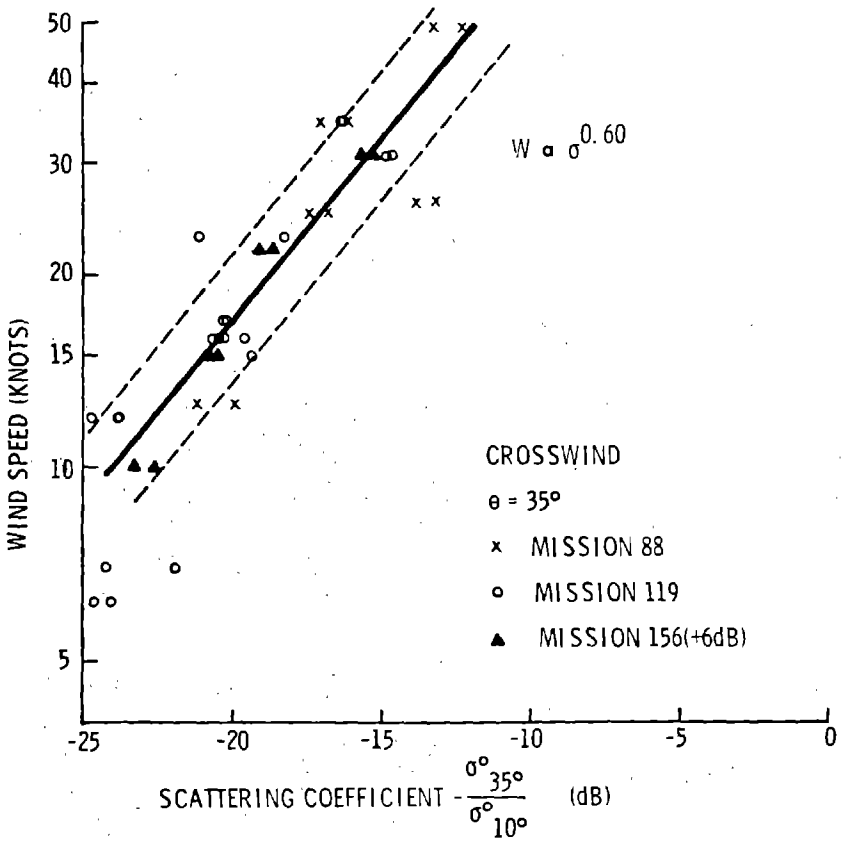

Figure 22. Anemometer calibration curve 13.3 GHz scatterometer 35° crosswind.

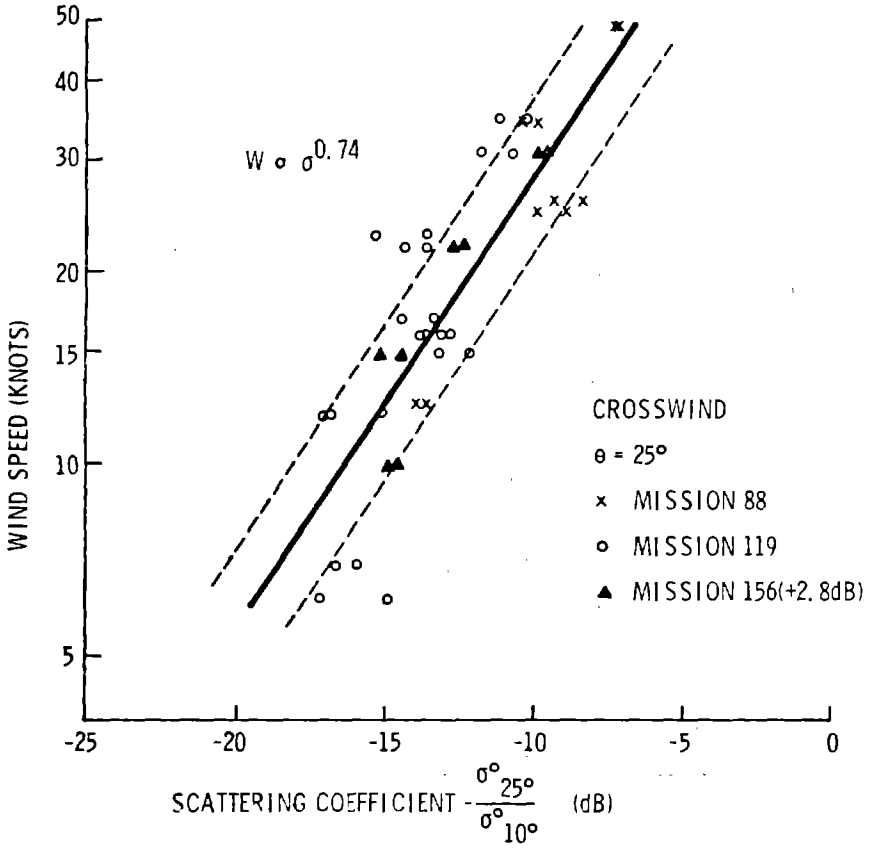

Figure 23. Anemometer calibration curve 13.3 GHz scatterometer 25° crosswind.

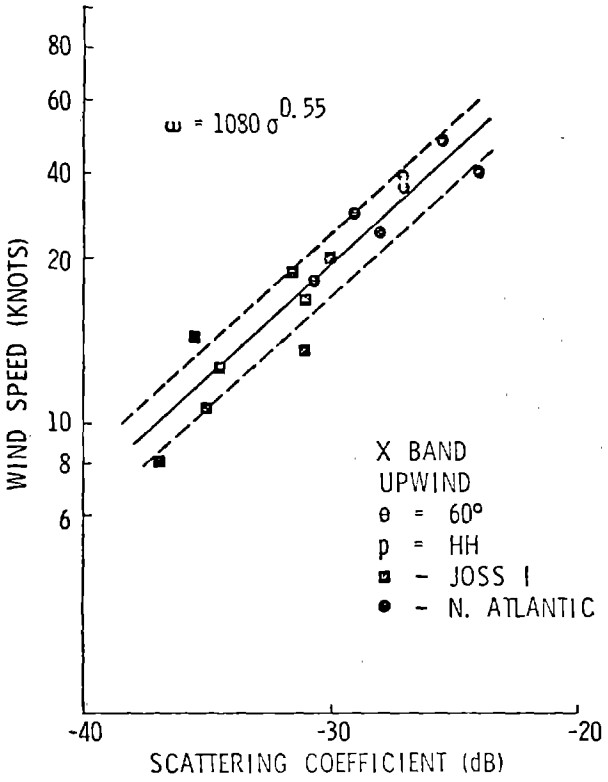

Figure 24. Wind speed as a function of scattering coefficient based on adjusted NRL data with standard deviation in wind estimate indicated.

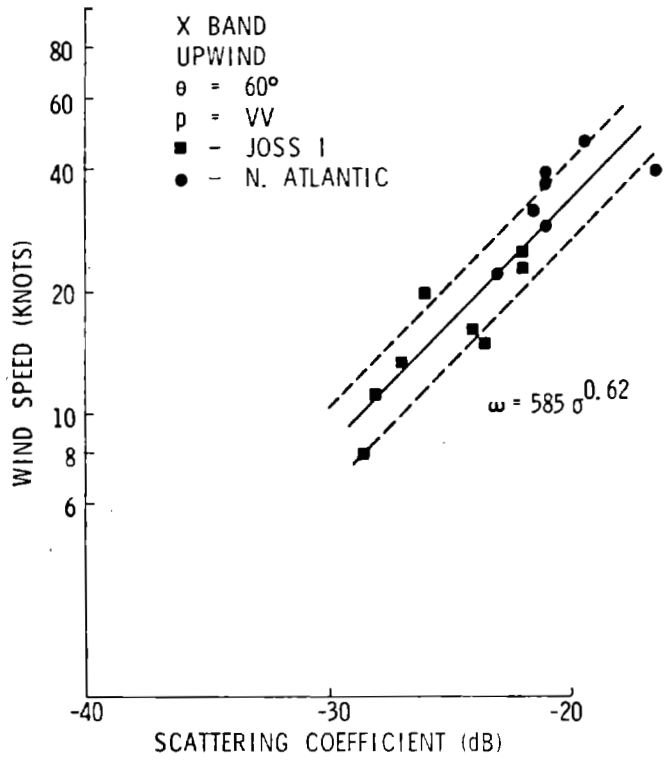

Figure 25. Wind speed as a function of scattering coefficient based on adjusted NRL data with standard deviation in wind estimate indicated.

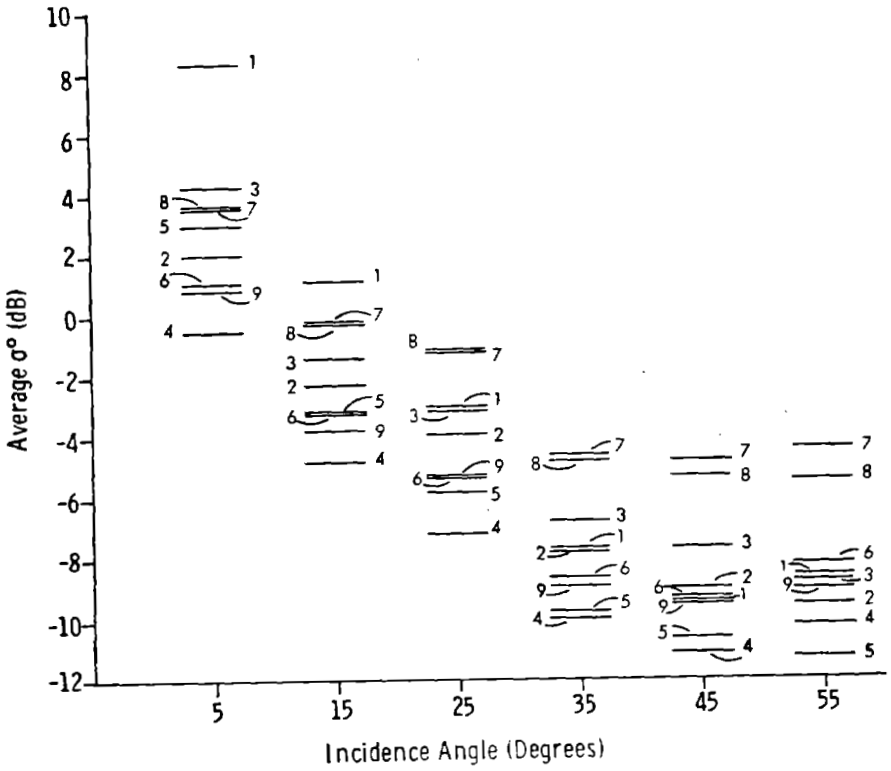

Figure 26. Spread of average σ° for nine ice-types versus angle.

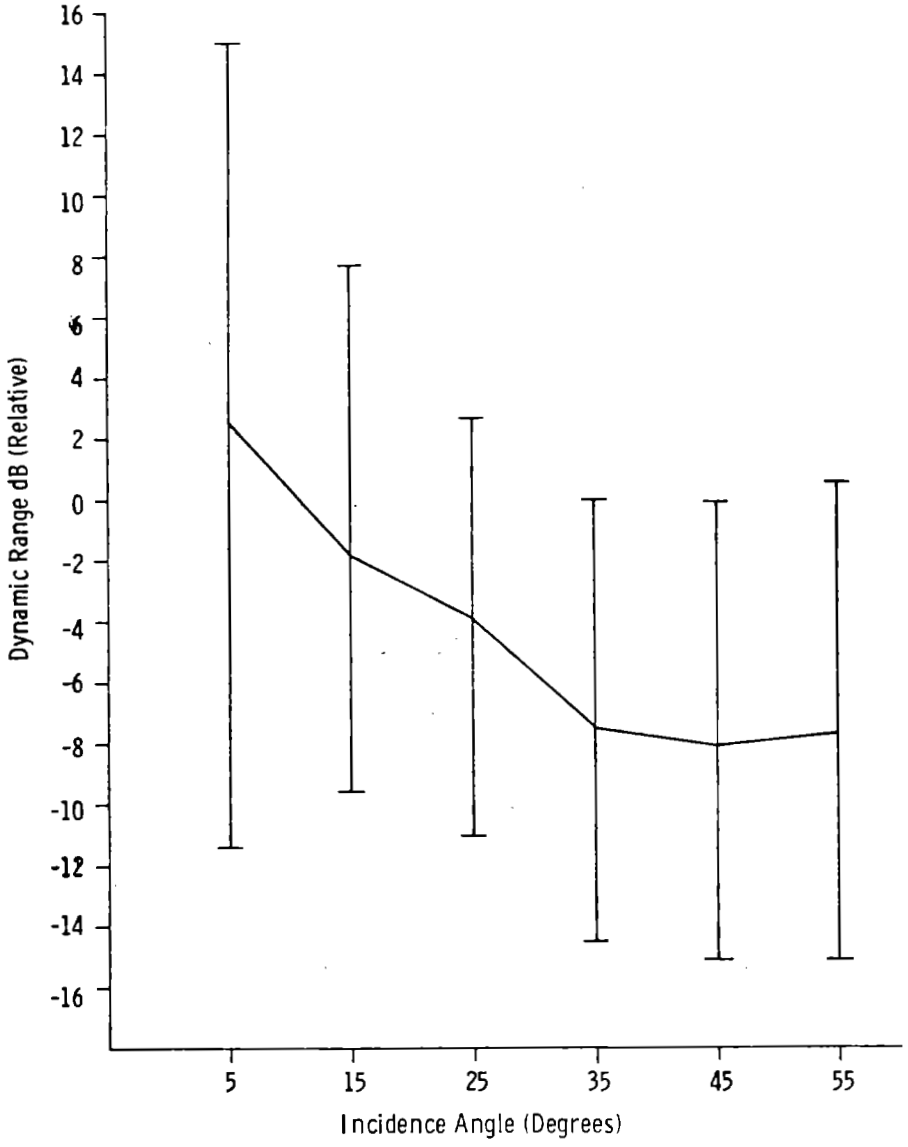

Figure 27. Dynamic range requirements for ice imager-radar.

AGRICULTURE SCATTEROMETRY PROGRAM

I. PRELIMINARY ANALYSIS OF MISSION 130 LINE OF 13.3 GHz DATA COMPLETED.

II. PROCESSING FORMAT SPECIFICATIONS COMPLETED FOR REMAINDER OF SCATTEROMETER DATA.
   1. SCALE OF DATA PLOT EQUAL TO PHOTOGRAPHIC SCALE.
   2. DATA PROCESSING SAMPLE LENGTH 0.3275 SECOND.
   3. ANGULAR RESOLUTION FREQUENCY BANDS SPECIFIED FOR +5°, THROUGH +60° WITH 5° INTERVALS.

III. ANALYSIS OF THE 400 MHz DATA FROM MISSIONS 130 AND 133 IN PROCESS.

IV. AWAITING 13.3 GHz DATA FROM MISSIONS 133, 153, 165, 168 AND THE REMAINDER OF LINES FROM MISSION 130.

Figure 28.

RESOLUTION: 10 m
SWATHWIDTH: 40 km
HEIGHT: 600 km
σ°: -25 dB
INCIDENCE ANGLE: 60°
SNR: 6 dB

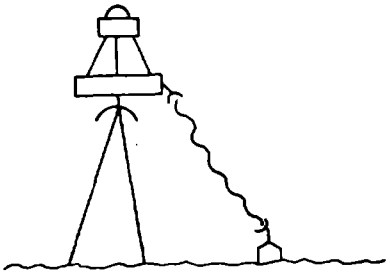

AVERAGE TRANSMITTED POWER: 125 W

POWER (INCLUDING SYSTEM & LOSSES) = 450 W

AVERAGE POWER FOR A 20% ORBITAL DUTY CYCLE: 90 W

30° INCIDENCE ANGLE GIVES A 8.4 dB SNR, ALLOWING 275 W AVERAGE POWER WITH ORBITAL AVERAGE OF 55 W.

Figure 29. Representative design for SLAR for small satellite. Poorer range resolution would allow lower power.

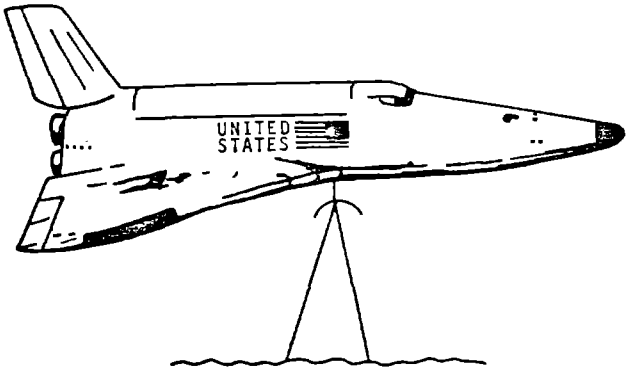

RESOLUTION: 10 m
SWATHWIDTH: 40 km
HEIGHT: 300 km
σ°: -25 dB
INCIDENCE ANGLE: 60°
SNR: 6 dB

FREQUENCY (GHz)	AVERAGE RADIATED POWER (W)	TRANSMITTER POWER (W)	POWER REQUIRED FOR WIDE-BAND AVERAGING (W) 200 MHz	400 MHz	SYSTEM POWER (W)
4	26	76	1020	2220	240
8	52	157	1870	3880	↓
10	64	192	2500	5200	
16	102	303	3980	8300	
		Σ 735	9350	19400	
POWER REQUIRED →		975	9590	19640	

Figure 30. Representative polychromatic/polypanchromatic radar system for large space craft.